

## Evaluation of mode-shape linearization for HFBB analysis of real tall buildings

K.T. Tse<sup>\*1</sup>, X.J. Yu<sup>1</sup> and P.A. Hitchcock<sup>2</sup>

<sup>1</sup>Department of Civil and Environmental Engineering, Hong Kong University of Science and Technology, Hong Kong

<sup>2</sup>CLP Power Wind/Wave Tunnel Facility, Hong Kong University of Science and Technology, Hong Kong

(Received March 5, 2011, Revised June 11, 2012, Accepted October 1, 2012)

**Abstract.** The high frequency base balance (HFBB) technique is a convenient and relatively fast wind tunnel testing technique for predicting wind-induced forces for tall building design. While modern tall building design has seen a number architecturally remarkable buildings constructed recently, the characteristics of those buildings are significantly different to those that were common when the HFBB technique was originally developed. In particular, the prediction of generalized forces for buildings with 3-dimensional mode shapes has a number of inherent uncertainties and challenges that need to be overcome to accurately predict building loads and responses. As an alternative to the more conventional application of general mode shape correction factors, an analysis methodology, referred to as the linear-mode-shape (LMS) method, has been recently developed to allow better estimates of the generalized forces by establishing a new set of centers at which the translational mode shapes are linear. The LMS method was initially evaluated and compared with the methods using mode shape correction factors for a rectangular building, which was wind tunnel tested in isolation in an open terrain for five incident wind angles at 22.5° increments from 0° to 90°. The results demonstrated that the LMS method provides more accurate predictions of the wind-induced loads and building responses than the application of mode shape correction factors. The LMS method was subsequently applied to a tall building project in Hong Kong. The building considered in the current study is located in a heavily developed business district and surrounded by tall buildings and mixed terrain. The HFBB results validated the versatility of the LMS method for the structural design of an actual tall building subjected to the varied wind characteristics caused by the surroundings. In comparison, the application of mode shape correction factors in the HFBB analysis did not directly take into account the influence of the site specific characteristics on the actual wind loads, hence their estimates of the building responses have a higher variability.

**Keywords:** HFBB; linear-mode-shape method; real tall building application; various site wind conditions; effects of surroundings

### 1. Introduction

The high-frequency base balance (HFBB) testing technique was developed in the early 1980s (Davenport and Tschanz 1981, Tschanz and Davenport 1983) and has become one of the most common wind tunnel testing techniques for predicting wind-induced forces for tall building design.

---

\*Corresponding author, Dr., E-mail: [timkttse@ust.hk](mailto:timkttse@ust.hk)

The fundamental premise of the HFBB technique is that the generalized wind forces exerted on a building can be estimated from the overturning and torsional moments measured using a lightweight and stiff model, in which only a building's external geometry is modeled. Predictions of dynamic loads and responses are determined analytically from the estimated generalized wind forces. For buildings with uncoupled linear mode shapes, the generalized wind forces are precisely equal to the measured base overturning moments and exact building dynamic responses can be directly determined by solving a set of generalized equations of motion. However, recent trends of irregular building shapes, increased building heights and more complex structural systems are likely to result in buildings having significantly nonlinear and/or three-dimensional (3D) mode shapes that have typically been treated through the application of mode shape correction factors.

Holmes (1987) derived mode shape correction factors for high and low correlations between any pair of fluctuating sectional forces at levels on a building by assuming that the wind force spectral densities were invariant with height. He then proposed a simple form of mode shape correction factor between the high and low correlation limits, which is suitable for use in a design code of practice. Boggs and Peterka (1989) considered mode shape correction factors for the upper limit of full correlation and assumed that the fluctuating forces varied with height as a power law. Xu and Kwok (1993) extended Holmes' mode shape correction factors to account for different variations of wind force spectral densities with height and distributions of wind forces with power law exponent of different values for alongwind, crosswind, and torsional excitations. Chen and Kareem (2004) derived another set of mode shape correction factors for fluctuating forces with an intermediate correlation of wind loads based on a presumed analytical wind loading model and a closed-form expression for wind load coherence.

It is evident that mode shape correction factors have been derived by adopting various analytical models and assumptions for the on-coming wind profile and mode shapes. Hence the correction factors inherently introduce other uncertainties in the generalized wind force predictions as they are not usually derived from the measured data of a particular test and therefore do not reflect the specific effects of the surroundings on wind flow affecting a building. Furthermore, the effects of surroundings on the accuracy of the generalized wind force predictions using mode shape correction factors have not been investigated in detail in the literature.

An alternative analysis methodology, referred to as the linear-mode-shape (LMS) method, has been recently developed to minimize the potential uncertainties in the estimation of generalized wind forces by "linearizing" the sway components of the 3D mode shapes without the need to assume or surmise the likely form of the wind load distributions. Therefore, the LMS method allows the exact computation of the sway components of the generalized wind forces while the torsional components of the generalized wind forces are still reliant on the application of more conventional mode shape corrections.

For the current study, the LMS method was initially evaluated and compared with the method using mode shape correction factors for a rectangular benchmark building, which was wind tunnel tested in isolation in a simulated open terrain. The generalized forces and responses computed using the LMS method and analysis methods with different mode shape correction factors were compared with the "exact" solutions, which were computed using the exact wind load distribution and mode shapes. A real tall building project, which is located in a heavily developed business district and surrounded by tall buildings and mixed terrain, was subsequently employed in this study to examine the effects of surroundings on the accuracy, versatility and reliability of the LMS method as well as the application of mode shape correction factors. The details of the wind tunnel

tests, results and performance of the methods under different wind loading environments due to the surroundings are outlined in this paper.

## 2. High Frequency Base Balance (HFBB) analysis using mode shape correction factors

### 2.1 Formulation of the equations of motion

A general matrix formulation of the equations of motion for a tall structure with rigid floor systems and subject to random wind loads can be expressed as

$$\mathbf{M}\ddot{\mathbf{x}} + \mathbf{C}\dot{\mathbf{x}} + \mathbf{K}\mathbf{x} = \mathbf{W} \quad (1)$$

where  $\mathbf{M}$  is the structural mass matrix in kg or kg·m<sup>2</sup>;  $\mathbf{C}$  is the proportional damping matrix in N·s/m or N·s·m/rad;  $\mathbf{K}$  is the stiffness matrix in N/m or N·m/rad;  $\mathbf{x}$  is the displacement vector in meters or radians; and  $\mathbf{W}$  is the wind excitation time history vector in N or N·m. The equations of motion are normally formulated at the storey mass centers because the resulting eigenvalue problem is computationally simpler (Li *et al.* 2007). Eq. (1) is transformed to a set of uncoupled modal equations by means of modal superposition, with mode shapes computed at the mass centers, as follows for the  $j$ th mode

$$m_j \ddot{\xi}_j(t) + c_j \dot{\xi}_j(t) + k_j \xi_j(t) = w_j(t) \quad (2)$$

where: generalized mass,  $m_j = \sum_i \left[ m(z_i) \phi_{jx}^2(z_i) + m(z_i) \phi_{jy}^2(z_i) + I(z_i) \phi_{j\theta}^2(z_i) \right]$ ;

generalized damping,  $c_j = 2m_j \omega_j \zeta_j$ ;

generalized stiffness,  $k_j = \omega_j^2 m_j$ ; and

generalized force,  $w_j = \sum_i \left[ w_x(z_i, t) \phi_{jx}(z_i) + w_y(z_i, t) \phi_{jy}(z_i) + w_\theta(z_i, t) \phi_{j\theta}(z_i) \right]$

where  $\xi_j(t)$  is the dimensionless generalized coordinate for the  $j$ th mode;  $m(z_i)$  and  $I(z_i)$  denote the mass and mass moment of inertia respectively for the  $i$ th storey at a height of  $z_i$ ;  $\phi_{jx}(z_i)$ ,  $\phi_{jy}(z_i)$ ,  $\phi_{j\theta}(z_i)$  are the values of the  $j$ th mode shape vector for the  $i$ th storey at a height of  $z_i$  along the  $x$  and  $y$  axes and about the mass center respectively;  $\omega_j$  and  $\zeta_j$  are the natural frequency and damping ratio respectively for the  $j$ th mode;  $w_x(z_i, t)$ ,  $w_y(z_i, t)$ , and  $w_\theta(z_i, t)$  are the time histories of wind force components impacting on the  $i$ th storey at a height of  $z_i$  along the  $x$  and  $y$  axes and about the mass center respectively.

The generalized mass, damping and stiffness in Eq. (2) can be computed using the storey masses, mass moments of inertia, natural frequencies and mode shapes output from a finite element analysis along with estimated modal damping ratios, whilst the generalized wind forces are determined from the base overturning and torsional moments measured from a wind tunnel HFBB test. For example, the generalized wind forces can be determined precisely for buildings with linear translational mode shapes and a constant torsional mode shape as follows:

$$w_j^b(t) \equiv C_{jx}^b \frac{M_{yy}(t)}{h} - C_{jy}^b \frac{M_{xx}(t)}{h} + C_{j\theta}^b M_{zz}(t) \quad (3)$$

where the superscripts  $b$  denote the quantities at the HFBB centers;  $C_{jx}^b$ ,  $C_{jy}^b$  and  $C_{j\theta}^b$  are the mode shape coefficients of  $x$ ,  $y$ , and  $\theta$  components at the top of the building for the  $j$ th mode;  $M_{xx}(t)$ ,  $M_{yy}(t)$  and  $M_{zz}(t)$  are the measured base overturning and torsional moments about  $x$ ,  $y$  axes and HFBB center respectively; and  $h$  is the building height.

## 2.2 Mode shape correction factors

Recent trends of increased building heights, irregular building shapes and more complex structural systems are likely to result in buildings having significantly nonlinear 3D mode shapes, which would induce considerable discrepancies in the prediction of generalized wind forces using Eq. (3). A number of studies have been conducted to address the effects of non-ideal mode shapes through the application of mode shape correction factors (i.e.,  $X_{jx}$ ,  $X_{jy}$ , and  $X_{j\theta}$ ) as expressed in Eq. (4). These studies have included Holmes (1987), Boggs and Peterka (1989), Xu and Kwok (1993), Holmes *et al.* (2003), Chen and Kareem (2004), and Lam and Li (2009).

$$w_j^b(t) = X_{jx} C_{jx}^b \frac{M_{yy}(t)}{h} - X_{jy} C_{jy}^b \frac{M_{xx}(t)}{h} + X_{j\theta} C_{j\theta}^b M_{zz}(t) \quad (4)$$

The derivation of mode shape correction factors by adopting various analytical models and assumptions for the on-coming wind profile and mode shapes is essentially the simplest and most direct quantitative method of compensating for the effects of non-ideal mode shapes in the estimation of generalized wind forces. Some of the mode shape correction factors, derived based on presuming the mean wind loading distribution as a power law function and different levels of correlation for the fluctuating components of wind load at different heights, are summarized in Table 1. Although these factors have been extensively used in wind tunnel laboratories, the method of using mode shape correction factors inherently introduces other uncertainties. Mode shape correction factors are typically generic and for the most part they are not derived from the measured data of a particular test, hence they may not reflect the specific effects of the surroundings on wind flow affecting a building.

Table 1 Correction factors for the estimation of generalized wind forces

	Low Correlation (Xu and Kwok 1993)	High Correlation (Boggs 1989)	Simplified (Holmes 1987)
Translation ( $X_{jx}, X_{jy}$ )	$\sqrt{\frac{3+2\alpha}{1+2\alpha+2\beta}}$	$\frac{2+\alpha}{1+\alpha+\beta}$	$\sqrt{\frac{4}{1+3\beta}}$
Twist ( $X_j$ )	$\sqrt{\frac{1+2\alpha}{1+2\alpha+2\beta}}$	$\frac{1+\alpha}{1+\alpha+\beta}$	$\sqrt{\frac{1}{1+2\beta}}$

$\alpha$  is the power law exponent of the mean wind velocity profile; and

$\beta$  is the mode shape power law exponent

### 3. Linear Mode Shape (LMS) method

It is evident that the uncertainties in the generalized wind force predictions are fundamentally associated with the nonlinearity of a building's mode shapes, instead of the actual wind force distribution. However, these uncertainties have usually been dealt with indirectly by presuming the wind force distribution as a power law function with an analytical spatial correlation, regardless of the likely influence of the specific surrounding buildings. As an alternative to the conventional application of mode shape correction factors, Tse *et al.* (2009) developed an analysis methodology, referred to as the linear-mode-shape (LMS) method, to minimize the potential uncertainties in the estimation of generalized wind forces by "linearizing" the sway components of the 3D mode shapes without the need to assume or surmise the likely form of the wind load distributions. Hence the LMS method is versatile and adaptable to a wide range of wind loading conditions and environments.

As shown in Eq. (3), the generalized wind forces are a composition of three terms, i.e.,  $x$ ,  $y$ , and  $\theta$ , integrating the product of the actual wind force and the mode shape values along the building height. The LMS method allows the exact computation of the sway components of the generalized wind force to be determined by establishing a new set of centers, referred to as the LMS centers, at which the translational mode shapes are "linearized" by axis transformations. The torsional component of the generalized wind force is still reliant on an appropriate selection of a torsional mode shape correction factor, as the twist mode shapes are independent of the axis transformation. It should be pointed out that the LMS method is based on the linearization of the translational mode shapes via axis transformation, which relies entirely on the existence of the twist component of the mode shape to alter the shape of the sway components. Hence the LMS method is not applicable to structurally-symmetric buildings or buildings with extremely high torsional stiffness, where the twist components of the mode shape are negligible. Detailed derivations and explanations of the LMS method were presented in Tse *et al.* (2009) and the analysis procedure is summarized as follows.

1. Linearize the 3D mode shapes and compute the locations of the LMS centers: in principle a mode shape which is highly nonlinear at the mass centers can be "linearized" through its transformation to other locations. When properly selected, there exist points along the building height at which the translational components are linear. The eccentricities of the  $j$ th mode LMS centers relative to the HFBB center are first of all determined using the following equations.

$$e_{jx}^l(z_i) = \frac{C_{jy}^l\left(\frac{z_i}{h}\right) - \phi_{jy}^b(z_i)}{\phi_{j\theta}^b(z_i)} \quad (5a)$$

$$e_{jy}^l(z_i) = \frac{-C_{jx}^l\left(\frac{z_i}{h}\right) + \phi_{jx}^b(z_i)}{\phi_{j\theta}^b(z_i)} \quad (5b)$$

where  $C_{jx}^l\left(\frac{z_i}{h}\right)$  and  $C_{jy}^l\left(\frac{z_i}{h}\right)$  are the predefined linear mode shapes.

2. Formulate the generalized equations of motion at the LMS centers: the generalized equations of motion, which are typically formulated at the mass centers or the HFBB center, are subsequently transformed to the LMS centers. For instance, the moments of inertia about a vertical axis at LMS centers are calculated using the Parallel-axis Theorem (Gere and Timoshenko 1997) with respect to the quantities at the mass centers.

$$m_j^l \ddot{\xi}_j(t) + c_j^l \dot{\xi}_j(t) + k_j^l \xi_j(t) = w_j^l(t) \quad (6)$$

In Eq. (6), the generalized mass, damping and stiffness are independent of the axis transformation and the location of the reference center. That means the quantities are the same as those at the mass centers.

3. Estimate the generalized wind force at the LMS centers for each mode

$$w_j^{l*} \cong \frac{C_{jx}^l}{h} M_{yy}(t) - \frac{C_{jy}^l}{h} M_{xx}(t) + C_{j\theta}^l \tilde{M}_{zz}(t) \quad (7)$$

where

$$\text{modified base torque, } \tilde{M}_{zz}(t) = X_{j\theta} M_{zz}(t) + \bar{e}_{jx}^l M_{xx}(t) + \bar{e}_{jy}^l M_{yy}(t)$$

$$\text{normalized weighted-average eccentricity, } \bar{e}_{jx}^l = \frac{\sum e_{jx}^l(z_i) \phi_{j\theta}^l(z_i)}{\sum z_i}$$

$$\text{normalized weighted-average eccentricity, } \bar{e}_{jy}^l = \frac{\sum e_{jy}^l(z_i) \phi_{j\theta}^l(z_i)}{\sum z_i}$$

4. Solve the generalized equations of motion for the modal coordinates: as indicated in Eq. (5), the values of the pair of eccentricities are unique for different modes because of their distinct mode shapes. Therefore, the LMS centers are different for each mode and the generalized equations of motion are solved for different coordinate systems for each mode.

5. Determine the building responses at the LMS centers: for instance, the storey translational displacements at the LMS centers can be obtained by multiplying the generalized coordinates with the linear mode shapes (i.e.  $C_{jx}^l \left( \frac{z_i}{h} \right)$  and  $C_{jy}^l \left( \frac{z_i}{h} \right)$ ).

6. Compute the building responses at locations of interest: the building responses at the LMS centers, which are defined specifically for the coordinate systems for each mode, are ultimately adjusted to one consistent coordinate system, e.g., at the mass centers, via axis transformation and subsequently superimposed to obtain the total building responses.

#### 4. Numerical verification: a benchmark building tested in isolation

It is common practice when evaluating HFBB analysis methods (e.g., Holmes 1987, Boggs and Peterka 1989, Yip and Flay 1995, Holmes *et al.* 2003 and Lam and Li 2009) to test a standard tall building model in isolation in a simulated open terrain. In the first phase of a numerical verification of the LMS method, the “exact” wind-induced response of the studied building structure was computed using a known wind pressure distribution measured from a wind tunnel pressure test, to provide an accurate benchmarking standard. The same set of pressure data were

then also used to synthesize base overturning and torsional moments that are equivalent to those that would be measured in a HFBB test, from which generalized forces and building responses were determined using the LMS method and the conventional HFBB methods involving the application of mode shape correction factors. The results were then compared with the “exact” values to examine their accuracy, robustness and reliability.

The second generation wind-excited benchmark building (Tse *et al.* 2007), which was employed as an example building in the initial numerical verification of the LMS method, is a 60-storey, 240 m tall reinforced concrete structure with a rectangular floor plan dimension of 24 m by 72 m throughout its height, as shown in Fig. 1. The building undergoes 3D lateral-torsional modes of vibration under wind excitation because of the asymmetrical structural configuration and the core setbacks, resulting in eccentricities between shear centers and mass centers.

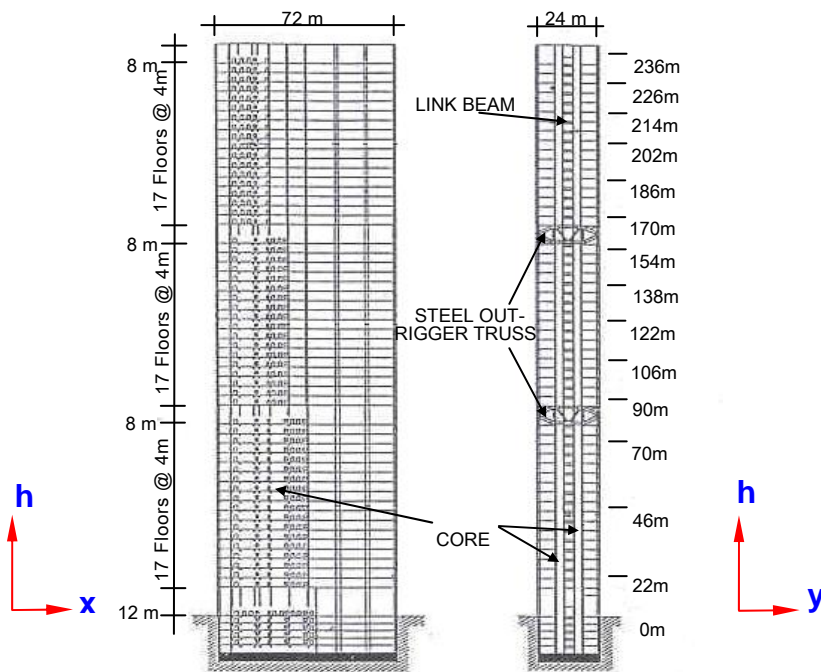


Fig. 1 The second generation wind-excited benchmark building

A 1:400 scale rigid model of the benchmark building was fabricated and tested at the CLP Power Wind/Wave Tunnel Facility (WWTF) at The Hong Kong University of Science and Technology (HKUST) to measure building surface pressures. The pressure model was tested in a simulated urban terrain, i.e., Terrain Category 3, as defined in AS/NZS 1170.2:2011 (Standards Australia 2011). Measurements were taken for five incident wind angles at  $22.5^\circ$  increments from  $0^\circ$  to  $90^\circ$ , where  $0^\circ$  corresponds to wind normal to the wide face of the building. The surface pressures measured from the test were integrated to derive base overturning and torsional moments and for subsequent use in the predictions of the generalized wind forces. Details of the structural configuration, finite element modeling, dynamic properties of the building, configuration of the

pressure test, the mean pressure coefficients on the surfaces of the building and the distributed mean wind forces along the building height are given in the work of Tse *et al.* (2007).

The external wind pressure time histories measured from the wind tunnel pressure test were first of all combined with the actual mode shapes at the mass centers to determine the “exact” generalized wind forces. The generalized equations of motion were subsequently solved to obtain the modal responses, which were combined with the mode shapes at the HFBB centers to determine the base overturning moment responses. The standard deviations of the resonant component of each mode and the resultant responses for a wind direction of  $0^\circ$  are summarized in Table 2. In the conventional HFBB analysis, the generalized wind forces were approximated using Eq. (4) and the mode shape correction factors listed in Table 1. The analysis procedures for the determination of base overturning moment responses followed the same method used for determining the “exact” values and results are given in Table 2 along with percentage differences relative to the “exact” values for ease of comparison.

Table 2 Standard deviation and percentage differences of base moment responses

		Standard deviation of base moment responses (MNm)							
		Mode	%	Mode	%	Mode	%	Resultant	%
		1	difference	2	difference	3	difference		difference
$M_x$	"Exact"	682	--	90	--	13.6	--	804	--
	LMS	683	0.0	94	4.4	40.9	200	805	0.1
	Low corr.	694	1.6	96	6.2	44.8	229	824	2.4
	High corr.	643	-5.8	89	-0.6	38.8	185	771	-4.1
	Simplified	688	0.8	94	4.5	40.8	200	815	1.3
$M_y$	"Exact"	136	--	315	--	6.8	--	368	--
	LMS	136	0.0	329	4.4	20.4	200	380	3.2
	Low corr.	138	1.6	334	6.2	22.3	229	403	9.6
	High corr.	128	-5.8	313	-0.6	19.3	185	364	-1.1
	Simplified	137	0.8	329	4.5	20.3	200	380	3.3
$M_z$	"Exact"	12.2	--	6.2	--	8.7	--	27.8	--
	LMS	12.2	0.0	6.5	4.4	26.1	200	37.1	33
	Low corr.	12.4	1.4	6.6	6.2	28.6	229	39.0	40
	High corr.	11.5	-5.8	6.1	-0.6	24.7	185	36	29
	Simplified	12.3	0.8	6.5	4.5	26.0	200	37.0	34

For the LMS method, the LMS centers were first of all determined using Eq. (5). The locations of the LMS centers, indicated by the eccentricities  $e'_x$  and  $e'_y$ , of the first three modes relative to the geometrical center of the building are depicted in Fig. 2, along with the nonlinear mode shapes at the mass centers and the predefined linear mode shapes at the LMS centers. It can be observed that the nonlinear translational mode shapes at the mass centers were “linearized” after being transformed to the LMS centers while the torsional modes were independent of the transformation of reference axes and remained unchanged. It is evident from Fig. 2 that the eccentricities of LMS centers can reach more than 1000m near the ground due to the diminishing twist component. It is

however that the huge eccentricities are to be compensated when multiplying with the twist component again to determine the normalized weight-average eccentricities, which are used in the generalized wind load estimation.

The generalized equations of motion were subsequently transformed to the LMS centers and the generalized wind forces were approximated according to Eq. (7) with the application of the “simplified” mode shape correction factors suggested by Holmes (1987) for torsional components. Because of the uniqueness of the LMS centers for each mode, the generalized equations of motion were solved for different coordinate systems for each mode, although the building responses were ultimately superimposed using one consistent coordinate system, in this case with reference to the HFBB center. The base overturning moment responses and the percentage differences are listed in Table 2.

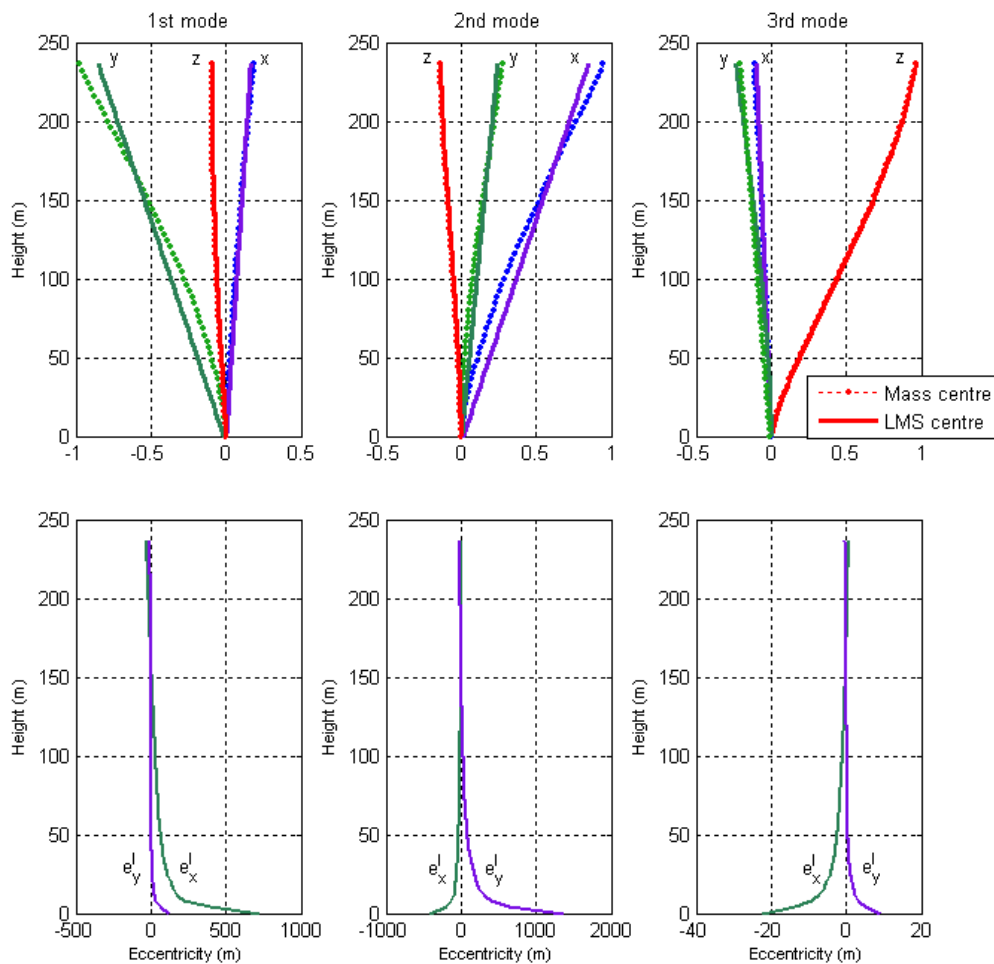


Fig. 2 Mode shapes at mass centers, linear mode shapes at LMS centers and locations of LMS centers

As indicated in Table 2, the percentage differences for the standard deviations of the resonant base moment responses for modes 1 and 2 were quite small for all methods considered in this study, among which the LMS methods and the application of simplified mode shape correction factors provide very accurate predictions with differences of less than 1% for mode 1. However, the building responses determined for mode 3 were more than double the magnitude of the “exact” responses for all methods, which is attributable primarily to the dominance of the torsional component of mode 3.

For the standard deviation of the resultant base overturning moment responses about the x and y axes (i.e.,  $M_x$  and  $M_y$ ) tabulated in the last column of Table 2, the LMS method generally offered the smallest positive percentage differences, implying that the estimated resultant building responses were the closest to the “exact” responses and yet slightly conservative. The results obtained using correction factors suggested by Holmes (1987), denoted as “simplified” in Table 2, had the second smallest percentage differences, followed by those for a “low correlation” of wind loads as proposed by Xu and Kwok (1993). On the contrary, analyses using correction factors for highly-correlated fluctuating forces resulted in negative percentage differences, which means the results were underestimated and the suggested correction factors were inappropriate for this particular building.

For the base torsional moment responses (i.e.,  $M_z$ ), each of the analysis methods considered in this study yielded values that were significantly different to the “exact” responses. This is due to the large uncertainties associated with determining the dominant torsional component of the modal force for mode 3 from the measured torque. It appears that the discrepancies of the estimated base torsional moment responses are likely to remain significant unless more rigorous torsional mode shape correction factors and/or analysis methods are derived. However, from a practical perspective, the torsional moment response is usually considerably smaller than the overturning moment responses for the majority of tall buildings.

## 5. Effects of surrounding buildings on generalized wind force predictions

One of the real challenges of a HFBB analysis method is to accurately estimate the generalized wind forces for an actual tall building, which is likely to be subjected to varied wind characteristics caused by the surroundings. Wind load distributions may also be significantly altered by nearby buildings, and significantly depart from the pattern of the approaching wind profile. Therefore, the results of a real tall building project, which is located in a heavily developed business district and surrounded by tall buildings and mixed terrain, were subsequently employed in this study to examine the effects of surroundings on the accuracy, versatility and reliability of the LMS method as well as the application of mode shape correction factors.

### 5.1 Details of the subject building and its surroundings

The subject building considered in this paper is a 36-storey residential tower on top of a 4-level commercial podium. The tower structure consists of load bearing walls and a simple beam and slab construction. Lateral wind loads acting on the tower are resisted by the core walls and load bearing walls of the tower. The tower structure is supported on a transfer beam sitting on the columns and walls of the podium. A typical floor plan, showing the reference axes, and an elevation of the building are presented in Fig. 3. The studied building has a height of

approximately 151 m above ground level over a small site coverage area of approximately 25 m by 13 m, resulting in an aspect ratio (H:W:D) of 12:6:1 and hence it is potentially wind sensitive.

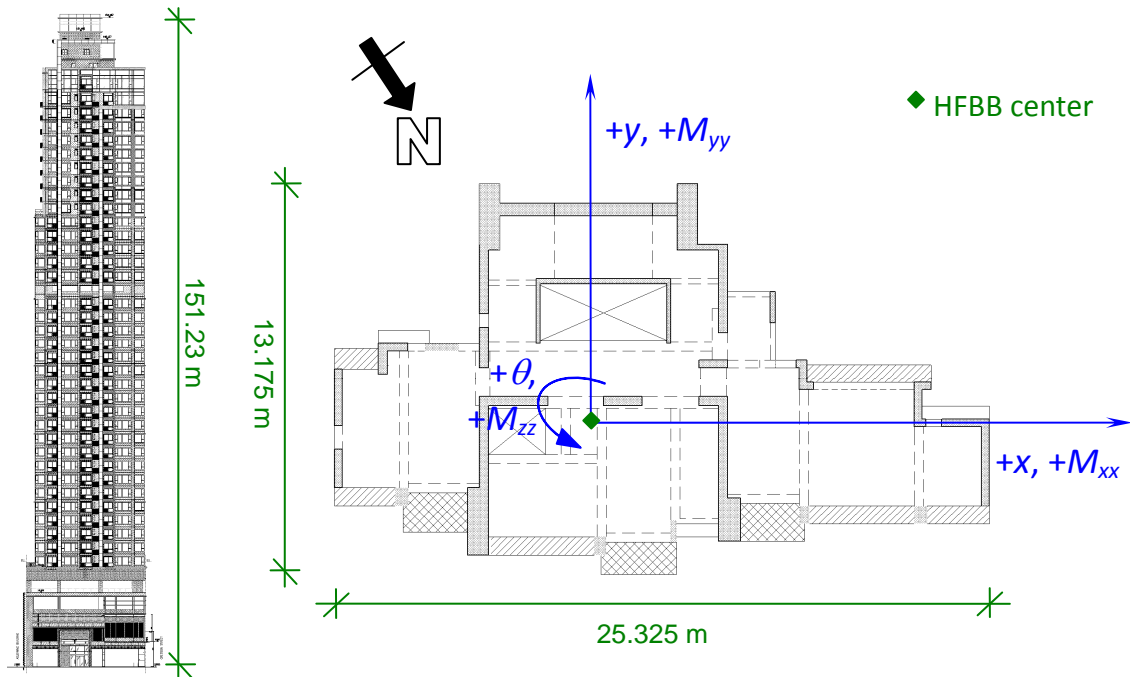


Fig. 3 Elevation and typical plan of the subject building

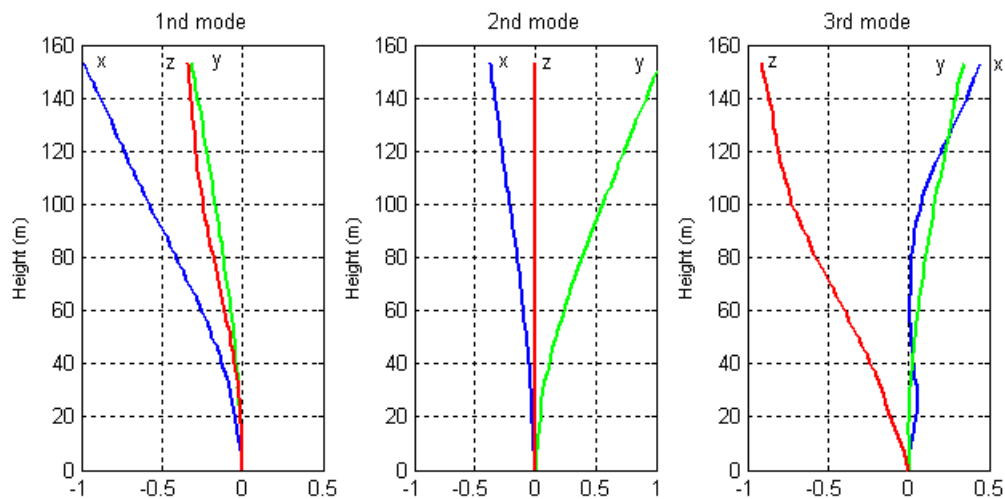


Fig. 4 Mode shapes of the subject building

The mode shapes corresponding to the first three modes of vibration, associated with the storey mass centers over the building height, are displayed in Fig. 4. It should be noted that the torsional mode shapes in Fig. 4 were multiplied by the overall radius of gyration (i.e., ~8.3 m) of the building to maintain dimensional consistency among the three ( $x, y, z$ ) components for the sake of presentation. The first mode of vibration has a dominant translational component along the  $x$  axis and a significant torsional component. The second mode is basically a translational mode of vibration (i.e., having a negligible torsional component) with a dominant component along the  $y$  axis. The third mode is a predominantly torsional mode of vibration with modest translational components. The natural frequencies of the first three modes were 0.238 Hz, 0.258 Hz and 0.429 Hz respectively.

The building site is close to the harbour front in Hong Kong. Fig. 5 shows the approximate location of the building and the general topography of the surroundings, which comprises complex mixtures of open water, urban and built-up terrain on the both sides of the harbor, and mountainous areas on Hong Kong Island to the south and in the New Territories to the north. A 1:2000 scale topographical study was undertaken to quantify the effects of local topography on mean and gust wind speeds approaching the site of the subject building. Results of the topographical study showed that the building has relatively open exposures towards the northeast and northwest directions, whereas it is sheltered from southerly winds by nearby mountains with peaks in excess of 400 m – 500 m. For the majority of wind directions, wind conditions approaching the building site were similar to wind flow over a large city center and were designated as condition A. For the remaining wind directions tested, wind conditions were similar to wind flow over urban terrain and designated as condition B. Mean wind speed and turbulence intensity profiles for the two approach conditions are presented in Fig. 6 along with power law functions that provided the best overall fit to the measured data.



Fig. 5 Location of the subject building and the surrounding topography

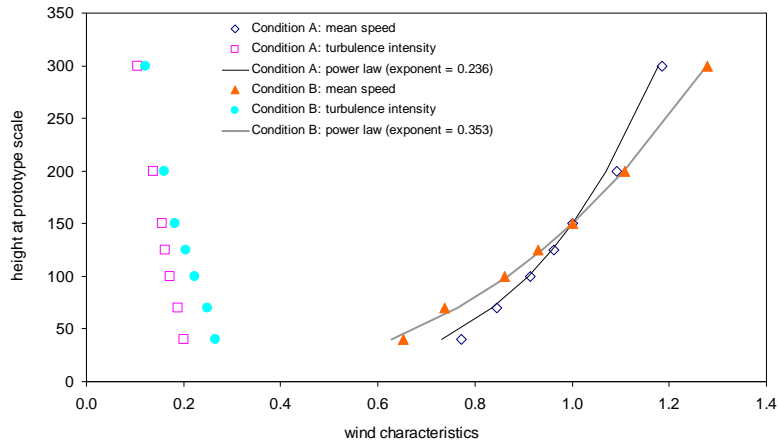


Fig. 6 1:400 scale wind characteristics: approaching wind conditions A and B

## 5.2 Wind tunnel HFBB test setup

A lightweight, 1:400 scale model of the subject building was mounted on a rigid base balance such that the overall mass and stiffness of the entire system produced sway and torsional natural frequencies that were well above the range of interest for the HFBB tests. The force balance was calibrated by applying a range of known static loads to the model prior to the wind tunnel testing to provide direct measurements of the wind loads. Measurements were taken for 36 wind directions at  $10^\circ$  intervals, for the full  $360^\circ$  azimuth, where a wind direction of  $0^\circ$  or  $360^\circ$  corresponds to an incident wind approaching directly from the north.

All known existing and planned surrounding buildings and topographical features within a radius of 500 m were modeled to the same linear scale and were included in the HFBB tests to simulate their effects on wind flows around the site and subject building. A map showing the coverage of the surrounding buildings is presented in Fig. 7, in which the buildings having heights significantly taller than the subject building are hatched in blue. The remaining areas are mainly slopes, open spaces and low-rise structures of height less than 100 m. For ease of reference, the distribution of approaching wind conditions is also illustrated in Fig. 7.

It is evident that the subject building was subjected to a wide range of wind loading environments, resulting from the combinations of the two different approaching wind conditions and the effects of the nearby surrounding buildings. For example, at a wind direction of  $20^\circ$ , the subject building is located downstream of a tall building complex; at a wind direction of  $100^\circ$ , the upper levels of the subject building were openly exposed to the approaching wind whereas the upstream buildings provided significant shielding to the lower levels; at wind directions of  $140^\circ - 150^\circ$ , the subject building was again situated downstream of a tall building complex and it was subjected to the less turbulent wind condition A. It is evident that, because of the complexity of surroundings, the wind loads experienced by the studied building were considerably altered and unlikely to follow the approaching wind profiles.



Fig. 7 Coverage of the 1:400 scale model

### 5.3 Determination of building responses using various HFBB analysis methods

For each of the 36 wind directions tested, the measured wind loads were combined with the dynamic properties of the subject building to evaluate analytically the dynamic loads and building responses corresponding to a return period of 50 years (Building Department, HKSAR 2004), in which structural damping ratios were assumed to be 1.5% of critical damping for modes 1 and 2 and 2% of critical damping for mode 3.

In the conventional HFBB analysis, the generalized wind forces were computed using three different sets of mode shape correction factors, as listed in Table 1, which are intrinsically in terms of the power law exponents of the building's mode shapes and the mean wind velocity profile. The mode shape power law exponents, which were obtained by performing a least-squares fit to the mode shape values, are summarized in Table 3. Similarly, the power law exponents of the mean wind velocity profiles were found to be 0.236 and 0.353 for wind conditions A and B, respectively. It worth noting that the measured mean wind speed profiles and the building's mode shapes, in particular the torsional component of mode 1 and the x-translational component of mode 3, were not satisfactorily fitted with a power law function. Hence uncertainties were inherently introduced in the calculations of mode shape correction factors and the subsequent generalized wind force predictions.

Table 3 Power law exponents of mode shapes

Mode	$\phi_x$	$\phi_y$	$\phi_z$
1	1.403	1.577	1.138
2	1.468	1.562	1.000
3	3.614	1.861	0.870

The three sets of mode shape correction factors, corresponding to low and high correlations of wind load and the simplified form, are given in Table 4. The low and high correlation mode shape correction factors had the largest and smallest values respectively, whilst the simplified factors were essentially between the two limits. Comparing the two approach wind conditions, the simplified mode shape correction factors are the same for both wind conditions since the calculations were independent of the power law exponent of the mean wind velocity profile. For the low and high correlation factors, the mode shape correction factors for wind condition A were always smaller than those for wind condition B because of the smaller power law exponent of the mean wind velocity profile for wind condition A.

Table 4 Mode shape correction factors for different wind conditions

Mode	low correlation			high correlation			simplified			
	$X_x$	$X_y$	$X$	$X_x$	$X_y$	$X$	$X_x$	$X_y$	$X$	
Condition A	1	0.901	0.866	0.627	0.847	0.795	0.521	0.876	0.835	0.552
	2	0.887	0.869	0.651	0.827	0.799	0.553	0.860	0.839	0.577
	3	0.632	0.817	0.677	0.461	0.722	0.587	0.581	0.779	0.604
Condition B	1	0.906	0.873	0.654	0.854	0.803	0.543	0.876	0.835	0.552
	2	0.893	0.876	0.678	0.834	0.807	0.575	0.860	0.839	0.577
	3	0.644	0.826	0.703	0.474	0.732	0.608	0.581	0.779	0.604

The peak base overturning moment response coefficients about the x-axis,  $C_{Mx}$ , was determined for each set of applied mode shape correction factors and the LMS method, as presented in Fig. 8. Largest wind-induced base moment response coefficients occurred at a wind direction of  $310^\circ$ , i.e., for wind approaching the site approximately from the northwest. The measured results for  $310^\circ$  exhibited enhanced turbulent energy, probably due to the presence of the upstream structures northwest of the subject building. The maximum and minimum peak overturning moment response coefficients for this wind direction are 1.38 and 1.11, obtained from the application of low and high correlation mode shape correction factors, respectively.

In terms of the accuracy of the different methods considered in this study, the results presented in Fig. 8 demonstrated a similar trend to the results of the benchmark building study tested in isolation. Comparable results were found for the simplified correction factor and the LMS method, providing values in between the upper and lower limits obtained from the application of low and high correlation mode shape correction factors, respectively. Furthermore, the results of the high correlation mode shape correction factors may underestimate the base moment responses for some

wind directions.

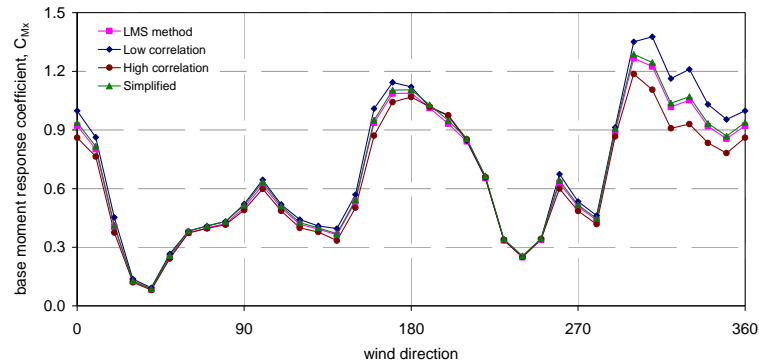


Fig. 8 Maximum base overturning moment response about the x-axis

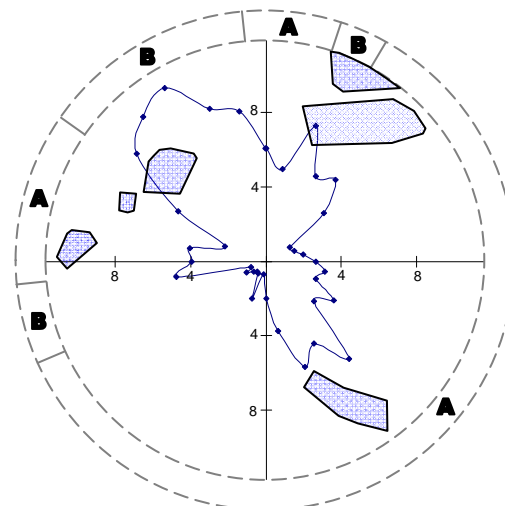


Fig. 9 Coefficients of variation (%) for  $M_x$  over the different HFBB analysis methods

It can also be seen from Fig. 8 that the variations of base moment response coefficients obtained using the different methods were higher at some directions, such as for  $300^\circ - 360^\circ$ . In order to more comprehensively investigate the performance of the various analyses under different wind conditions due to the surroundings, the values of the base overturning moment coefficients together with their “coefficient of variation”, defined as the standard deviation normalized by the averaged value (i.e.,  $\sigma_M / \bar{M}$ ) and expressed as a percentage, are given in Table 5 and Fig. 9. Fig. 9 also includes the distribution of wind conditions and the locations of tall building complexes for better illustration. It is evident that the applicability and suitability of mode shape correction factors in the HFBB analysis were significantly influenced by the wind conditions and the characteristics of the surrounding terrain. For the wind directions of  $50^\circ - 130^\circ$  and  $180^\circ - 260^\circ$ , the subject building was relatively exposed as the surrounding buildings were shorter and the coefficients of variation were relatively small, with values as low as 1% or less. However, the

coefficients of variation were considerably higher when the subject building was located downstream of a tall building complex, e.g.,  $20^\circ - 40^\circ$ ,  $140^\circ - 160^\circ$ ,  $270^\circ$ , and  $310^\circ - 350^\circ$ , and particularly under the influence of the higher turbulent wind condition B.

Table 5 Maximum base overturning moment response coefficients and coefficients of variation

angle	LMS method	Base moment response coefficient, $C_{Mx}$			Simplified	Coefficients of variation (%)
		Low correlation	High correlation			
0	0.92	1.00	0.86	0.94	6.07	
10	0.80	0.86	0.76	0.82	5.03	
20	0.40	0.45	0.38	0.41	7.74	
30	0.13	0.14	0.12	0.13	5.30	
40	0.08	0.09	0.08	0.09	5.72	
50	0.25	0.27	0.24	0.26	3.99	
60	0.37	0.38	0.37	0.38	1.48	
70	0.40	0.41	0.40	0.41	1.62	
80	0.42	0.43	0.42	0.43	1.99	
90	0.50	0.52	0.49	0.51	2.65	
100	0.62	0.64	0.60	0.63	3.17	
110	0.50	0.52	0.49	0.51	2.81	
120	0.42	0.44	0.40	0.43	4.19	
130	0.39	0.41	0.38	0.40	3.33	
140	0.36	0.40	0.33	0.37	6.85	
150	0.53	0.57	0.50	0.54	5.09	
160	0.94	1.01	0.87	0.95	6.02	
170	1.09	1.14	1.04	1.10	3.81	
180	1.09	1.12	1.07	1.11	2.03	
190	1.01	1.02	1.02	1.03	0.69	
200	0.93	0.97	0.98	0.95	2.15	
210	0.84	0.84	0.85	0.86	0.77	
220	0.65	0.66	0.66	0.66	0.74	
230	0.34	0.34	0.34	0.34	0.84	
240	0.25	0.25	0.25	0.26	1.18	
250	0.34	0.34	0.34	0.34	0.85	
260	0.63	0.67	0.60	0.64	4.82	
270	0.51	0.53	0.49	0.52	3.94	
280	0.44	0.46	0.42	0.45	4.10	
290	0.89	0.91	0.87	0.90	2.30	
300	1.27	1.35	1.19	1.29	5.35	
310	1.22	1.38	1.11	1.24	8.97	
320	1.02	1.16	0.91	1.04	10.12	
330	1.05	1.21	0.93	1.07	10.76	
340	0.92	1.03	0.83	0.93	8.73	
350	0.85	0.95	0.78	0.87	8.17	
360	0.92	1.00	0.86	0.94	6.07	

## **6. Conclusions**

The analysis procedures of a recently developed HFBB method, referred to as the linear-mode-shape (LMS) method, were illustrated in this paper. The main advantage of the method is that its accuracy does not require knowledge of the wind load distributions and hence it is expected to be adaptable in typical tall building environments where wind loading conditions are significantly influenced by the surroundings.

The LMS method was evaluated in two different stages to exam its reliability, versatility and accuracy, in particular under varied wind loading environments. In the initial stage, a series of wind tunnel pressure tests was conducted to determine the wind load distribution on the benchmark building tested in isolation. "Exact" wind-induced responses were computed and used as a benchmarking standard for comparison with the LMS method and common HFBB analysis methods that use mode shape correction factors to account for non-ideal mode shapes. The LMS method generally offered the most accurate and slightly conservative base overturning moment response predictions among the methods considered in this paper, enabling substantial improvements in the prediction of the generalized wind forces and the estimation of translational structural responses.

The same analysis methods were further evaluated using a real tall building project in Hong Kong to study the effects of surrounding buildings on their accuracy. The results demonstrated that the accuracy and reliability of HFBB analysis methods depend significantly on the terrain characteristics of the nearby surroundings. When the subject building was relatively exposed to the approaching wind, consistent results among various methods were obtained. However, high coefficients of variation were found for the wind directions at which the tested building was downstream of a tall building complex, especially under highly turbulent winds. Therefore, mode shape correction factors should be applied with caution in HFBB analyses when tall building complexes exist in the surrounding proximity.

It should be noted that the paper is at this time primarily of academic interest whose intent is to demonstrate a new approach from a novel and alternative viewpoint. The LMS is not recommended for commercial use at this time. This is because, while the LMS method provides an alternative to the estimation of structural responses, the uncertainties due to the mode shape correction factors used in the torsional components of the generalized wind force are still present. In other words, the accuracy of the LMS method to predict the generalized wind force is reliant on the selection of an appropriate torsional mode shape correction factor. In addition, the LMS method is based on the linearization of the translational mode shapes via axis transformation, which relies entirely on the existence of the twist component coupled in translational mode shapes. Therefore the LMS method would possibly lose the applicability when the building is structurally-symmetric or extremely stiff in torsion, where the twist components of the mode shape are infinitesimal and potentially cause errors in the computation of LMS centers and the subsequent structural response estimations.

## **Acknowledgements**

This research project is funded by a Research Grants Council of Hong Kong Central Allocation Grant (Project CA04/05.EG01). Thanks also go to the staff of the CLP Power Wind/Wave Tunnel Facility at HKUST for their assistance in this project.

## References

- Boggs, D.W. and Peterka, J.A. (1989), "Aerodynamic model tests of tall buildings", *J. Eng. Mech. - ASCE*, **115**(3), 618-635.
- Buildings Department (HKSAR) (2004), Code of Practice on Wind Effects in Hong Kong.
- Chen, X. and Kareem, A. (2004), "Equivalent static wind loads on buildings: new model", *J. Struct. Eng. - ASCE*, **130**(10), 1425-1435.
- Davenport, A.G. and Tschanz, T. (1981), "The response of tall buildings to wind", *Proceedings of the 4th U.S. Nat. Conf. of Wind Engineering*, July 27-29, Seattle, Washington, U.S.A.,
- Gere and Timoshenko, S. (1997), *Mechanics of materials*, PWS Publishing Company.
- Holmes, J.D. (1987), "Mode shape correction factors for dynamic response to wind", *Eng. Struct.*, **9**(3), 210-212.
- Holmes, J.D., Rofail, A. and Aurelius, L. (2003), "High frequency base balance methodologies for tall buildings with torsional and coupled resonant modes", *Proceedings of the 11th International Conf. on Wind Engineering*, June 1-5, Lubbock, Texas, U.S.A.
- Lam, K.M. and Li, A. (2009), "Mode shape correction factors for wind-induced dynamic responses of tall buildings using time-domain computation and wind tunnel tests", *J. Sound Vib.*, **322** (4-5), 740-755.
- Li, H.N., Yi, T.H., Yi, X.D. and Wang, G.X. (2007), "Measurement and analysis of wind-induced response of tall building based on GPS technology", *Adv. Struct. Eng.*, **10**(1), 83-93
- Standards Australia (2011), *Australian/New Zealand Standard, Structural design actions Part 2: Wind actions*, AS/NZS 1170.2:2011, Standards Australia, Sydney, N.S.W, Australia
- Tschanz, T. and Davenport, A.G. (1983), "The base balance technique for the determination of dynamic wind loads", *J. Wind Eng. Ind. Aerod.*, **13**(1-3), 429-439.
- Tse, K.T., Hitchcock, P.A. and Kwok, K.C.S. (2009), "Mode shape linearization for HFBB analysis of wind-excited complex tall buildings", *Eng. Struct.*, **31**(3), 675-685.
- Tse, K.T., Kwok, K.C.S., Hitchcock, P.A., Samali, B. and Huang, M.F. (2007), "Vibration control of a wind-excited benchmark tall building with complex lateral-torsional modes of vibration", *Adv. Struct. Eng.*, **10**(3), 283-304.
- Xu, Y.L. and Kwok, K.C.S. (1993), "Mode shape corrections for wind tunnel tests of tall buildings", *Eng. Struct.*, **15**(5), 387-392.